AD-A171 128 ELECTROMAGNETIC SENSOR ARRAYS FOR NONDESTRUCTIVE EVALUATION AND ROBOT CONTROL(U) SRI INTERNATIONAL MENLO PARK CA A J BAHR ET AL. 31 OCT 85 AFOSR-TR-86-0511 1/1

UNCLASSIFIED F49620-84-K-0011 F/G 14/2 NL

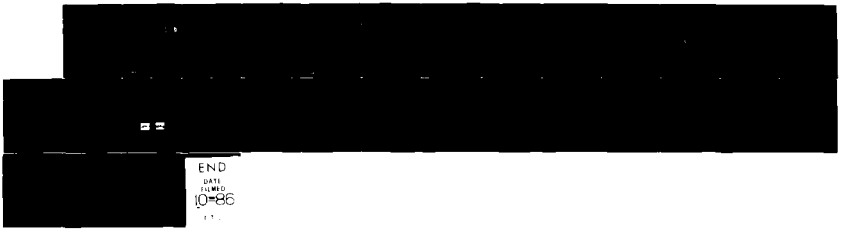

END

DATE FILMED

10-86

DTIC

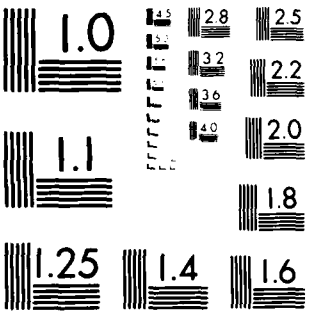

ROCOPY RESOLUTION TEST CHART
NATIONAL BUREAU OF STANDARDS 1963-A

(2)

ELECTROMAGNETIC SENSOR ARRAYS FOR NONDESTRUCTIVE EVALUATION AND ROBOT CONTROL

By: A. J. BAHR A. ROSENGREEN

October 1985

Annual Technical Report
Covering the period 1 September 1984 - 31 August 1985

7

Prepared for:

AIR FORCE OFFICE OF SCIENTIFIC RESEARCH
DIRECTORATE OF ELECTRONIC AND SOLID STATE SCIENCES
BOLLING AIR FORCE BASE, BUILDING 410
WASHINGTON, D.C. 20332

Attention: MAJOR J. W. HAGER
Program Manager, AFOSR/Electronic & Materials Sciences

CONTRACT F49620-84-K-0011

SRI Project 7711

Approved for public release; distribution unlimited.

SRI International
333 Ravenswood Avenue
Menlo Park, California 94025
(415) 326-6200
Cable: SRI INTL MPK
TWX: 910-373-2046

UNCLASSIFIED

SECURITY CLASSIFICATION OF THIS PAGE

REPORT DOCUMENTATION PAGE

1a. REPORT SECURITY CLASSIFICATION UNCLASSIFIED	1b. RESTRICTIVE MARKINGS NONE
2a. SECURITY CLASSIFICATION AUTHORITY	3. DISTRIBUTION/AVAILABILITY OF REPORT APPROVED FOR PUBLIC RELEASE; DISTRIBUTION UNLIMITED
2b. DECLASSIFICATION/DOWNGRADING SCHEDULE	
4. PERFORMING ORGANIZATION REPORT NUMBER(S) ANNUAL REPORT No. 1	5. MONITORING ORGANIZATION REPORT NUMBER(S) AFOSR-TR- 86-0511
6a. NAME OF PERFORMING ORGANIZATION SRI INTERNATIONAL 6b. OFFICE SYMBOL (If applicable)	7a. NAME OF MONITORING ORGANIZATION Same as 6a
6c. ADDRESS (City, State and ZIP Code) 333 Ravenswood Avenue Menlo Park, California 94025	7b. ADDRESS (City, State and ZIP Code) Same as 6c
8a. NAME OF FUNDING/SPONSORING ORGANIZATION USAF, AFSC 8b. OFFICE SYMBOL (If applicable) AFOSR/NE	9. PROCUREMENT INSTRUMENT IDENTIFICATION NUMBER CONTRACT No. F49620-84-K-0011
8c. ADDRESS (City, State and ZIP Code) Building 410 Bolling AFB, DC 20332	10. SOURCE OF FUNDING NOS. ELEMENT NO. 61102F; PROJECT NO. 2306/A2; TASK NO. A2; WORK UNIT NO.
11. TITLE (Include Security Classification) Electromagnetic Sensor Arrays for Nondestructive Evaluation & Robot Contro.	
12. PERSONAL AUTHOR(S) A. J. Bahr and A. Rosengreen	
13a. TYPE OF REPORT Annual 13b. TIME COVERED FROM 840901 TO 850831	14. DATE OF REPORT (Yr., Mo., Day) 1985 October 31 15. PAGE COUNT 26
16. SUPPLEMENTARY NOTATION	

17. COSATI CODES			18. SUBJECT TERMS (Continue on reverse if necessary and identify by block number)
FIELD	GROUP	SUB. GR.	Sensor, nondestructive evaluation, robotics, electromagnetic, imaging
09	F		

19. ABSTRACT (Continue on reverse if necessary and identify by block number)

The objective of this research program is to develop the theoretical models, design methodology, and technology needed for optimum application of near-field electromagnetic sensor arrays in nondestructive evaluation (NDE) and robot control. This program is a collaborative effort by SRI and Stanford University. This report summarizes SRI's contribution to the program's first year research activities.

To aid in understanding how best to analyze and control the spatial-frequency content in the field configuration generated by an array, most of this ~~first~~ year's effort ~~at SRI~~, focused on obtaining experimental measurements of the relative spatial distributions defined by the responses of inductive eddy-current reflection probes to surface steps and surface-breaking rectangular slots in aluminum plates. In particular, a commercial reflection probe (Nortec SPO-2065) and an SRI-constructed, five-coil, air-core reflection probe have been used to interrogate such surface discontinuities. The data obtained using the five-coil probe compare favorably with the results of a theory developed at Stanford University.

20. DISTRIBUTION/AVAILABILITY OF ABSTRACT UNCLASSIFIED/UNLIMITED ☒ SAME AS RPT. ☐ DTIC USERS ☐	21. ABSTRACT SECURITY CLASSIFICATION UNCLASSIFIED
22a. NAME OF RESPONSIBLE INDIVIDUAL Lt. Col. Joseph Hager	22b. TELEPHONE NUMBER (Include Area Code) 202-767-4933 22c. OFFICE SYMBOL NE

DD FORM 1473, 83 APR EDITION OF 1 JAN 73 IS OBSOLETE.

UNCLASSIFIED

SECURITY CLASSIFICATION OF THIS PAGE

A second part of SRI's effort has been to survey thin-film recording-head technology to assess its applicability to the fabrication of inductive sensor arrays. Besides devices employing high-permeability magnetic films, this survey also included those based on magnetoresistance and the Hall effect. The interim findings of this survey are reported here.

A third task at SRI is the study and development of data-processing algorithms for improving the resolution of electromagnetic sensor arrays. One class of such algorithms is based on deconvolution. The results of some preliminary work in this area are reported.

SRI International

ELECTROMAGNETIC SENSOR ARRAYS FOR NONDESTRUCTIVE EVALUATION AND ROBOT CONTROL

By: A. J. BAHR A. ROSENGREEN

October 1985

Annual Technical Report
Covering the period 1 September 1984 - 31 August 1985

Prepared for:

AIR FORCE OFFICE OF SCIENTIFIC RESEARCH
DIRECTORATE OF ELECTRONIC AND SOLID STATE SCIENCES
BOLLING AIR FORCE BASE, BUILDING 410
WASHINGTON, D.C. 20332

Attention: MAJOR J. W. HAGER
Program Manager, AFOSR/Electronic & Materials Sciences

CONTRACT F49620-84-K-0011

SRI Project 7711

Approved for public release; distribution unlimited.

Approved by:

LAWRENCE E. SWEENEY, JR., *Director*
Remote Measurements Laboratory

DAVID A. JOHNSON, *Executive Director*
Engineering Research Group

SRI INTERNATIONAL, 333 Ravenswood Avenue, Menlo Park, California 94025
(415) 326-6200, Cable: SRI INTL MPK, TWX: 910-373-2046

SRI International

CONTENTS

ILLUSTRATIONS

I INTRODUCTION

The objective of this research program is to develop the theoretical models, design methodology, and technology needed for optimum application of near-field electromagnetic sensor arrays in nondestructive evaluation (NDE) and robot control. This program is a collaborative effort by SRI and Stanford University, supported by separate contracts. This report summarizes SRI's contribution to the program's research in this first year.

A basic requirement for this work is the ability to analyze and control the spatial-frequency content in the field configuration associated with the electromagnetic sensor array. To understand how best to satisfy this requirement, SRI focused work this first year on obtaining experimental measurements of the relative spatial distributions defined by the responses of inductive eddy-current reflection probes to surface steps and surface-breaking rectangular slots in aluminum plates. A commercial reflection probe [Nortec SPO-2065] and an SRI-constructed, five-coil, air-core reflection probe were used to interrogate such surface discontinuities. The data obtained using the five-coil probe were compared with the results of a theory developed at Stanford University.[1]

A second part of SRI's effort this past year has been to survey thin-film recording head technology to assess its applicability to the fabrication of inductive sensor arrays. The survey is to include devices that employ high-permeability magnetic films and those based on magnetoresistance and the Hall effect. The interim findings of this survey are reported here.

The third component of the research activities at SRI in this program is the study and development of data-processing algorithms to be used to improve the resolution of electromagnetic sensor arrays. One class of such algorithms is based on deconvolution. Work has just begun on this problem, so only some preliminary thoughts can be discussed at this time.

II RESEARCH STATUS

A. Measurements

An automated system was built to acquire the amplitude and phase of a sensor array's output voltage as the array is scanned in a plane [x and y] under computer control.[2] Using stepping motors, the sensor array (or workpiece) was moved along in raster fashion with a minimum step size of 0.002 inches (or multiples thereof). A Nortec NDT-18 eddyscope was used as source and receiver, and the digitized data were stored on magnetic tape for off-line processing. (The NDT-18 eddyscope is an analog instrument containing a synthesized source that can be tuned from 50 Hz to 5 MHz and can be used with reflection probes as well as with absolute and differential probes.) Software was developed to permit displaying the data in several ways, including perspective plots and contour plots.

In the first series of experiments using this system, a Nortec SPO-2065 probe was used to investigate the relative step responses of a reflection-type probe. The drive coil in this probe has about a 0.1-inch outer diameter. The sensor array is composed of a differential pair of small D-shaped coils located side by side within the inner diameter of the drive coil. Based on the dimensions of these sensing coils, one would expect this probe to have a spatial resolution of about 0.040 in. (corresponding to a spatial frequency of 25 $in.^{-1}$, or 1.0 mm^{-1}).

The amplitude and phase responses of this probe to a series of 0.004-in.-deep (0.1-in. wide) steps milled in an aluminum plate were measured. The measured amplitude response illustrated two of this probe's resolution characteristics: (1) each step was resolved along the scan line, as expected, and (2) the variation of the vertical distance of each step from the probe was also easily resolved. In the experiment, this vertical distance varied between 0.004 and 0.016 in. (0.004 in. of liftoff occurred outside the step region). Generally, without resorting to any data processing, the distance over which vertical resolution is

obtained should be about equal to the transverse resolution of the sensor array. These data confirm this general behavior.

A reflection probe in which the drive and sense coils are essentially coplanar (in some reflection probes the coils are coaxial) is linearly polarized; that is, the probe's step response is maximum when the scan direction is perpendicular to the edge of the step and is aligned with a line that passes through the centers of the sense coils (parallel polarization), and it will be minimum (ideally zero) when the probe is rotated by 90° (perpendicular polarization).

The response of the Nortec reflection probe to a curved step illustrates this polarization-dependent behavior (Figure 1). The important implication of this characteristic of reflection probes is that, by combining data sets from both polarizations, the direction of the edge (or the orientation of a crack) with respect to the scan direction can be estimated. Thus, for example, by feeding this information back to the scan controller, the sensor array could be made to follow an edge.

To provide both polarizations in a single probe, a five-coil air-core reflection probe was designed at Stanford University and fabricated at SRI. The coils were made relatively large to minimize construction difficulties. The cross section of the probe is shown in Figure 2. As can be seen, the probe contains four coils in its sensor array. In experiments carried out to date, only two of the sense coils were operative at any one time, with diametrically opposed coils connected as a differential pair.

For one experiment, three slots of differing depths (0.125, 0.250, and 0.375 in.) were milled into an aluminum plate. The slots were each 0.125-in. wide and 1.5-in. long and were placed side by side, 1-in. apart. Figure 3 shows the results of scanning across them with the five-coil probe (only one sensor-pair active). The perspective plot of the results obtained by scanning across the 0.250-in.-deep slot shows a typical differential-probe response in the x direction, and a typical absolute-probe response in the y direction. This behavior is the result of the linear polarization characteristic discussed above. Stated another way, the x

response is determined by the spatial frequencies associated with the sensor array, while the y response is determined by the spatial frequencies associated with the drive coil.

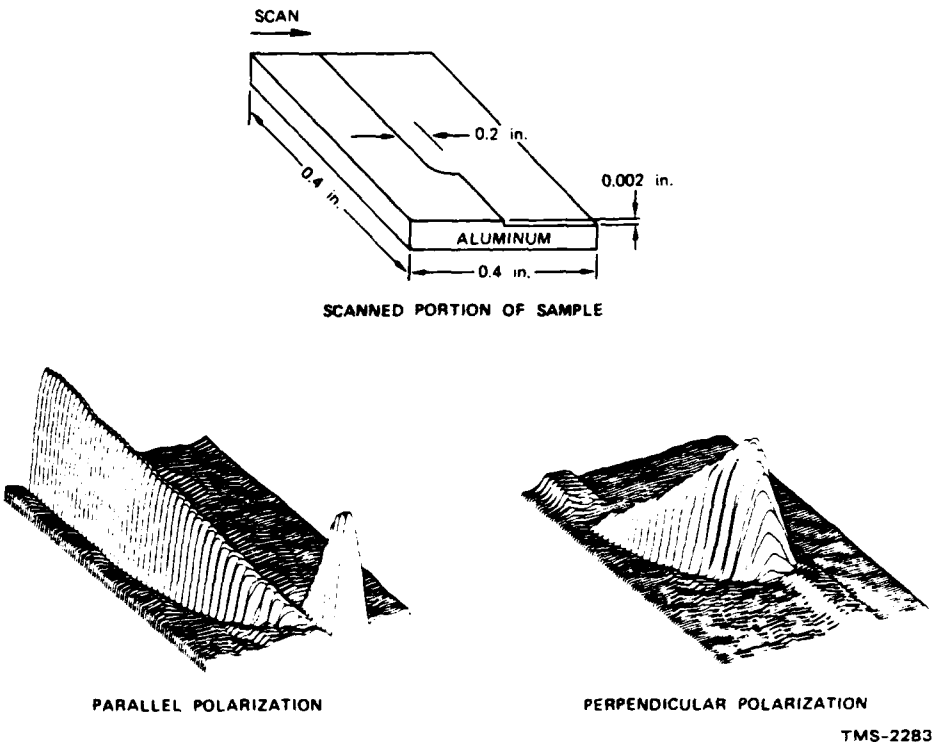

Figure 1. Response of a reflection probe to a curved step.

The line scan through the midpoints of these slots illustrates both the transverse resolution and the depth resolution of the probe. The transverse resolution appears to be about ±0.125 inches, and the depth resolution rapidly deteriorates for depths greater than 0.125 inches. These numbers are consistent with the dimensions of the probe. One objective of future work will be to develop data processing techniques that will improve the image quality produced by such a sensor array.

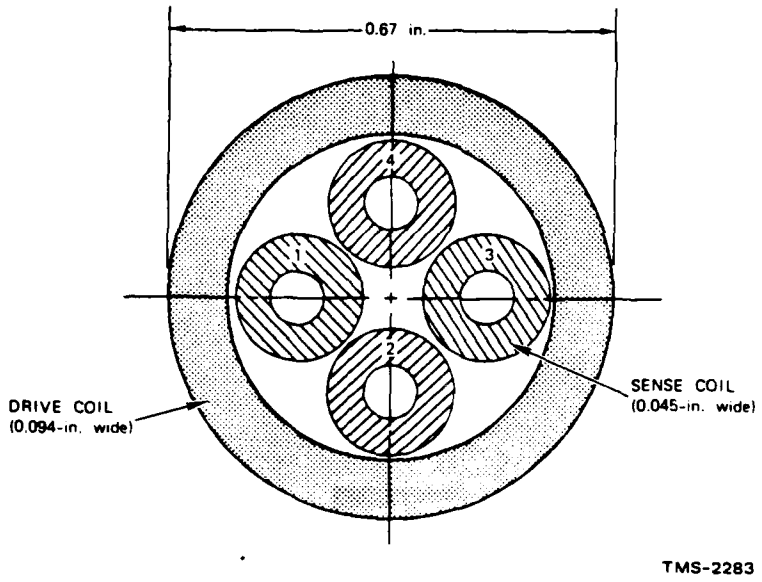

Figure 2. Cross section of a five-coil reflection probe.

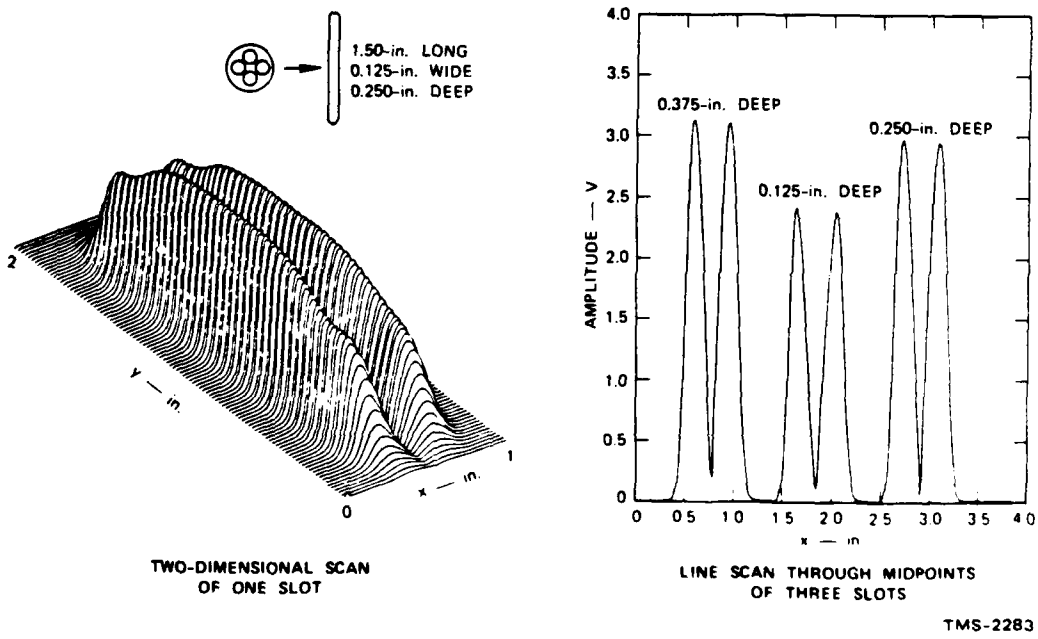

Figure 3. Slot response of a five-coil reflection probe - - 500 kHz.

A second experiment was conducted to obtain data for comparison with theoretical results computed at Stanford University.[1] In this experiment, the five-coil probe was used to make a series of five perpendicular scans across a 0.004-in. step in an aluminum plate. The orientation of the probe differed in each of these scans; starting from the point at which the line through the centers of the differential pair of sense coils was aligned with the scan direction (designated 0°), the probe was rotated in steps of 22.5° through 90° (designated 90°).

The experimental results are shown in Figure 4. As expected, the maximum measured step response is obtained at 0°, and the response decreases as the probe is rotated towards 90°. Comparisons with theory are shown for probe orientations of 0° and 67.5°. Since the NDT-18 is an

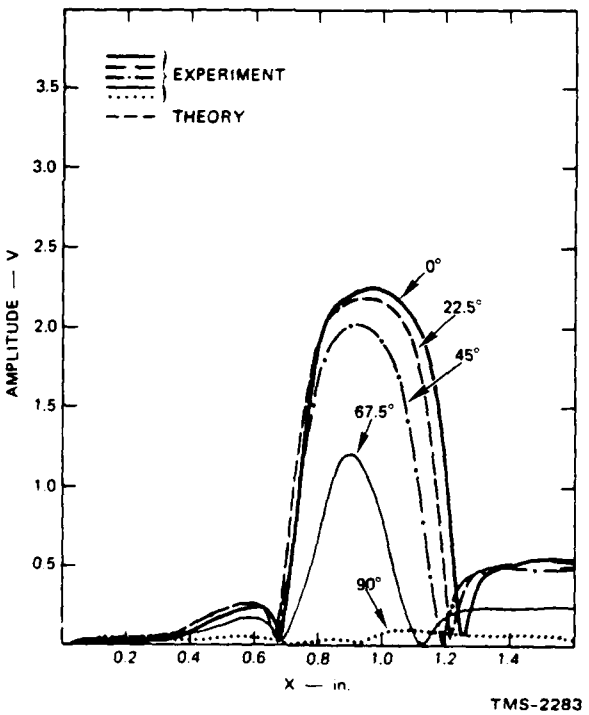

Figure 4. Step response as a function of probe orientation relative to the edge - - 500 kHz.

uncalibrated instrument, the theoretical and experimental data were matched at the maximum of the 0° scan. With this single-point calibration, the shapes of the main theoretical and experimental step responses are seen to agree very well, and the peak amplitudes of the 67.5° responses are in excellent agreement. The minor differences between theory and experiment outside the main step-response region are thought to be due to an interaction between the step and the drive coil that is not included in the theory.

B. Technology Survey

The spatial resolution of a conventional recording head consisting of a magnetic yoke encircled by wire-wound coils is about 1 mm when used as an eddy-current sensor.[3] To improve the resolution, smaller inductive sensors are needed. One approach would be to take advantage of the thin-film technology currently under development for manufacturing recording heads. Therefore, a literature study was initiated to assess the status of thin-film recording-head technology and its relevance to electromagnetic sensor arrays. The study was limited to two sources that contain a major part of the open literature on this technology: (1) the IEEE Transactions on Magnetics, and (2) the Proceedings of the Annual Conference on Magnetism and Magnetic Materials published in the Journal of Applied Physics.

The survey revealed that two devices might be candidates for application in an electromagnetic sensor array: the read-write thin-film magnetic head for computer disks, which is a thin-film version of the standard recording head, and the thin-film magnetoresistive device used for reading magnetic tapes.

1. Thin-Film Magnetic Head

The thin-film magnetic head is basically a two-dimensional version of the standard recording head that consists of a magnetic yoke and wire-wound coils. Figure 5 shows a typical example of a thin-film recording head. The drawing is sectioned to show the head's layered structure.

The first step in the fabrication of this head is the deposition of a magnetic film on a ceramic substrate. The film forms the bottom layer of the magnetic yoke amd is made from magnetic materials such as permaloy, Co-Zr, or mu metal. Next, the magnetic material is covered with an insulating layer of SiO_2. After this step, alternating layers of a conductor and a SiO_2 insulator are deposited. Each metal layer is etched into a spiral coil configuration using masks of photoresist. The spiral coils are interconnected through etched openings in the SiO_2 layers. Finally the top layer of the magnetic yoke is deposited. This layer makes contact at one end with the bottom layer of the yoke, while the other end is separated from the bottom layer by one or several layers of SiO_2. The number of insulating layers determines the dimension of the recording gap. The gap is typically between 0.2 μm to 2 μm wide and 0.01 mm to 0.5 mm long. (In the head shown in Figure 5, the gap is 2-μm wide and 0.41-mm long.) A special beveling technique is used during etching of the coils which allows the second-layer coil to be inlaid in the gaps of the first-layer coil, etc. This technique produces a planar coil surface which allows many layers to be deposited on top of each other.

More commonly, a single-layer coil is used like the one shown in Figure 6. This coil has 17 turns, an inductance of 200 nH, and a resistance of 15 Ω. However, the technology associated with the device shown in Figure 5 is to be preferred when compactness of the coil is critical.

When it is used in a hard-disk drive for computers, the thin-film head floats on an air cushion about 0.2 μm above the disk surface. The disk rotates at high speed, which produces flux reversals in the thin-film gap at frequencies above 1 MHz. The frequency response of the head shown in Figure 5 is close to being flat from 1 MHz to 4 MHz, with an output voltage of 3.3 mV to 3.6 mV. Above 4 MHz, the frequency response decreases by about 3 dB per octave. No data were available below 1 MHz, but the response would be expected to fall with decreasing frequency because the induced voltage in the coil is proportional to frequency.

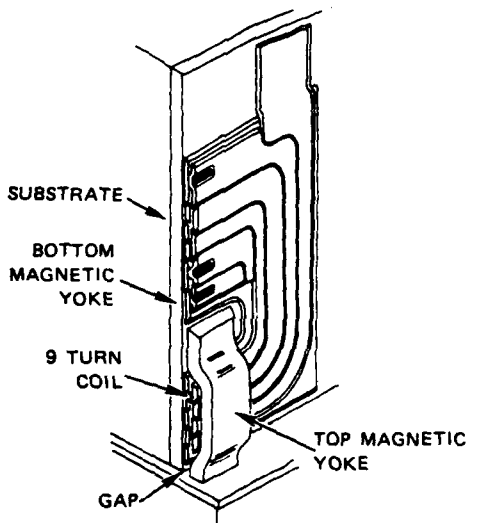

SOURCE: Reference 4 TMS-2283

Figure 5. Thin-film head with multilayer coil (9 turns).

(a) x2000 (b) x5000

SOURCE: Reference 5 TMS-2283

Figure 6. Single-layer coil with 17 turns. Coil dimensions: 3.5-μm wide, 3.2-μm thick, 1.5-μm space.

The thin-film head senses the change of the magnetic field in the gap. For application in a hard-disk drive, the head's spatial resolution in the scan direction is about equal to the gap width. However, for application to crack or edge detection in a metal plate, the gap width must be aligned parallel with the crack or edge for maximum sensitivity. In this case, the spatial resolution is determined by the length of the top magnetic yoke, but, since the length can be made as small as 10 μm, this is not a severe limitation. The real problem in using a thin-film magnetic head is that its height above the surface must be of the order of the gap width. Scanning a sensor array at a lift-off distance of less than 1 μm is simply not practical in NDE or robotics applications. The lift-off distance probably cannot be smaller than about 25 μm (1 mil). Thus, larger gap widths would be required. Since the gap width in a thin-film head is determined by a thin SiO_2 film whose maximum thickness is limited to a few micrometers, this fabrication method would no longer be applicable. Furthermore, increasing the gap width may require an increase in the number of coil turns. To keep the coil resistance at a reasonable level, the dimensions of the coil would have to be increased, and thus we are forced out of the domain of thin-film technology.

In summary, it appears that the technology for fabricating practical inductive sensor arrays with the desired high spatial resolution falls in a gray area between thin-magnetic-film technology and wire-wound-coil technology, with neither technology particularly well-suited to the purpose. However, as we shall see in the following sections, magnetic thin-film technology may still be applicable if the need for coils is abandoned and is replaced by other techniques for measuring a magnetic field.

2. Thin-Film Magnetoresistive Head

The thin-film magnetic head responds well to the high rates of flux change produced by high density disks spinning at high velocities, but its sensitivity is too low to be useful with the slow tape speeds used in audio and digital recording. For this reason, another type of thin-film head is presently under development in industry that does not depend on

the rate of flux change for its sensitivity. Instead, it measures the magnetic field itself by using the magnetoresistive effect in a thin film of permalloy (NiFe, 81%/19%). Figure 7a shows a sketch of such a film with its magnetization, M, along the length of the film. The film has an isotropic resistivity, ρ, that depends on the angle, ϑ, that the current makes with the magnetization, M. This directional dependence is given by [6,7]

$$\rho = \rho_o - \Delta\rho \sin^2\vartheta \quad , \tag{1}$$

where ρ_o is the film resistivity obtained when the current and magnetization are aligned, and $\Delta\rho$ is the maximum possible change in resistivity. The quantity $\Delta\rho$ depends on the magnitude of I and is, at most, 2% or 3% of ρ_o. If a current, I, is sent through the film, the voltage across the film will change if a magnetic field, H, is applied perpendicularly to M because the angle, θ, will change by a small increment, $\Delta\vartheta$, given by

$$\sin(\Delta\theta) = \frac{H}{H_o} \quad , \tag{2}$$

where H_o is the saturation field equal to the sum of the anisotropy field and the demagnetizing field. Therefore, by measuring the voltage across the film, the element can be used as a magnetic field sensor.

To reduce the effect of the nonlinearity implied by Eqs. (1) and (2), the sensor usually is constructed so that $\theta = \pm 45°$. This is done by using the so-called barber-pole configuration[6-8] shown in Figure 7b, in which strips of thin gold film are deposited at a 45° angle to the magnetization direction on top of the permalloy film. Because of the low resistivity of gold, the current in the permalloy film between the gold strips will take the shortest path between them, i.e., the current will flow in a direction 45° to the magnetization direction. To further reduce the nonlinearity, a symmetric structure like the one in Figure 7c is often used. In this configuration, the nonlinearity caused by the factor $\sin^2\theta$ cancels out. A multisensor array using 32 sensor elements

of this type has been reported.[8] The length of each sensor in this array was 100 μm and the output voltage was linear for magnetic fields up to 10 A/cm, where the corresponding output voltage was 2mV for an applied current of 50 mA.

Compared with the thin-film magnetic sensor, the thin-film magnetoresistive sensor is very attractive because of its simple structure. However, it is strictly a reading sensor that requires a separate drive field. At this point it is not clear what the best method is for creating such a drive field, and how sensitive the sensor will be at a reasonable lift-off distance. Further investigation is required.

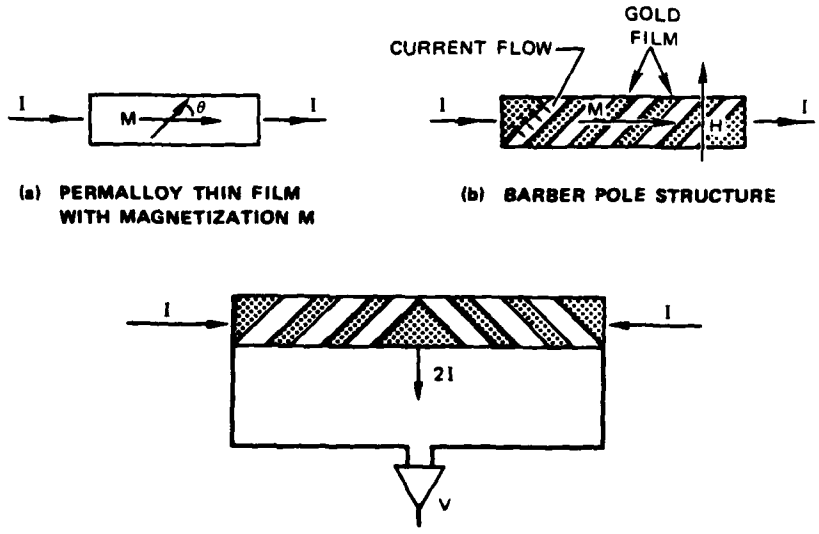

Figure 7. Magnetoresistive field sensor.

3. Summary and Discussion of Future Work

The brief literature search on the use of magnetic thin-film technologies for the fabrication of inductive sensor arrays with high spatial resolution suggested two possible types of magnetic recording heads: (1) the thin-film magnetic read-write head, and (2) the thin-film magnetoresistive read head.

The thin-film magnetic head is a thin-film version of a standard head made using a magnetic yoke and wire-wound coils. With a magnetic gap of 0.5 μm to 1 μm, the thin-film head is typically used at a height (liftoff) of about 0.2 μm above the recording medium. For the practical liftoff distances of interest in this research program (25 μm or more), the required dimensions of the yoke and the number of turns in the coils fall outside the present capabilities of thin-film technology.

The magnetoresistive sensor, which relies on anisotropic resistivity, has a simple structure that should be easy to produce in an array configuration, with a high degree of spatial resolution. However, since it is a read-only device, a separate drive field would have to be provided.

Possible drive methods will be investigated and estimates of the sensor sensitivity will be calculated as part of this evaluation. If results of these studies are promising, the availability of magnetoresistive sensors will be determined. If these sensors are not yet available in a form compatible with our requirements, the technology of magnetoresistive thin films will be further studied to determine the possibility of fabricating them at SRI or Stanford University.

In addition to these efforts, other magnetic-field sensing devices such as Hall-effect sensors will be studied. Capacitive sensors will be evaluated at Stanford University.

C. Quasistatic Near-Field Imaging

The basic transverse spatial resolution of an electromagnetic sensor array is determined by the physical dimensions of an array element. However, it should be possible to improve this resolution by taking advantage of the knowledge of the array's response to a highly localized surface

perturbation. This approach is analogous to using knowledge of the impulse response of a two-port electrical network to find the form of an excitation waveform that produces a given output waveform. The "impulse" response of a sensor array can be determined either theoretically or by experiment. The following is a discussion of a theoretical approach to the problem. Work has also been initiated to evaluate the use of only experimental data in the deconvolution process, but this work is in an early stage and is not discussed here.

1. Lorentz Reciprocity--Bistatic System

The theoretical approach to this problem is based on an application of Lorentz's reciprocity theorem to a probe system. This approach was pioneered in eddy-current nondestructive testing by Auld, et al.[9] Figure 8 shows a general, bistatic system consisting of driver probe, sensor probe, and a test piece to be inspected.

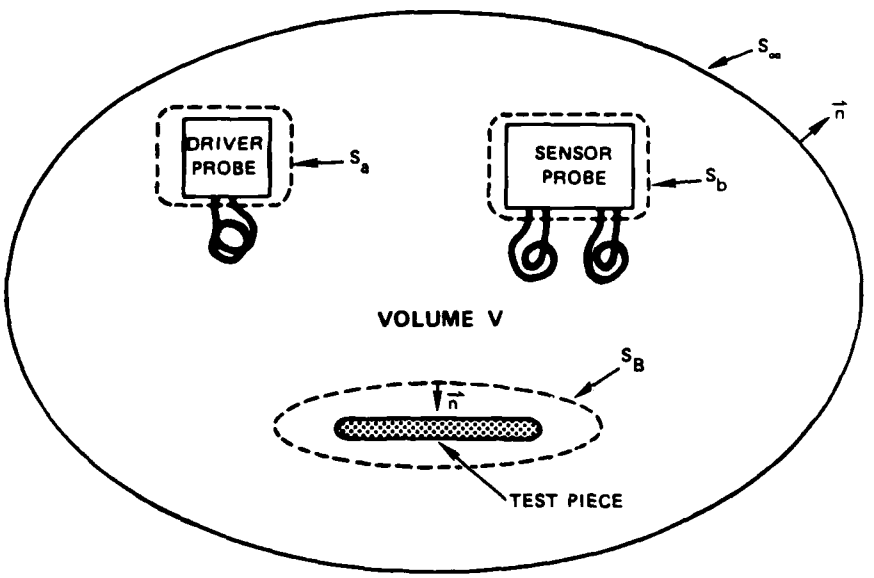

Figure 8. Bistatic probe geometry for application of Lorentz reciprocity theorem.

The relevant form of the reciprocity theorem is

$$\oiint (\vec{E}_1 \times \vec{H}_2 - \vec{E}_2 \times \vec{H}_1) \cdot \hat{n}\, ds = 0 \quad , \tag{3}$$

where the integral is taken over the total enclosing surface of the sourceless volume V. The key to the derivation is to define two distinct physical cases that are relevant to the problem:

Case 1--Driver probe "a" is excited (port 1) and the test piece is in a perturbed state.

Case 2--Sensor probe "b" is excited (port 2) and the test piece is in its unperturbed reference state.

These two cases correspond to subscripts 1 and 2 in Eq. (3). By applying appropriate boundary conditions,[9] one is left with an integral over the surface surrounding the test piece, S_B, and across ports 1 and 2. The surface S_B can be inside the test piece as well. The terminal conditions at the two ports are defined in Figure 9.

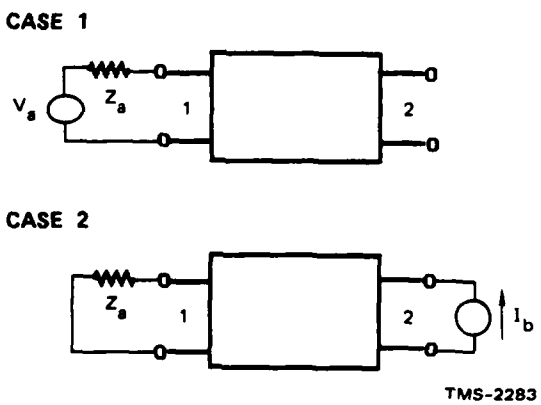

Figure 9. Terminal conditions at the probe ports.

It has been assumed in Case 1 that port 1 is connected to a finite-impedance source and that port 2 is connected to a high impedance (∞) detector. This is the case, for example, for an NDT-18 eddyscope.

In terms of terminal voltages and currents, Eq. (3) becomes

$$V_1^{(1)} I_1^{(2)} - V_1^{(2)} I_1^{(1)} + V_2^{(1)} I_b = -\oiint_{S_B} (\vec{E}_1 \times \vec{H}_2 - \vec{E}_2 \times \vec{H}_1) \cdot \hat{n} \, dS_B \quad , \quad (4)$$

where the boundary conditions $I_2^{(1)} = 0$ and $I_2^{(2)} = I_b$ have been used. Now, in terms of two-port z parameters, the first two terms in the left-and side of Eq. (4) can be written as

$$(z_{11}^{(1)} - z_{11}^{(2)}) \cdot I_1^{(1)} I_1^{(2)} - z_{12}^{(2)} \cdot I_1^{(1)} I_b \quad .$$

Also,

$$V_1^{(2)} = z_{11}^{(2)} I_1^{(2)} + z_{12}^{(2)} I_b \quad . \quad (5)$$

Assume, now, that the probe system is differentially balanced in Case 2. Hence, $V_1^{(2)}$ must be zero and it follows from Eq. (5) that

$$I_1^{(2)} = 0 \text{ and } z_{12}^{(2)} = 0 \quad ,$$

which makes the first two terms in the left-hand side of Eq. (4) equal to zero. Finally, if one defines a normalized voltage $v = V_2^{(1)}/V_a$, Eq. (4) becomes

$$v = -[1/(V_a I_b)] \oiint_{S_B} (\vec{E}_1 \times \vec{H}_2 - \vec{E}_2 \times \vec{H}_1) \cdot \hat{n} \, dS_B \quad . \quad (6)$$

This equation relates the observable, v, to the tangential fields on the surface S_B.

2. Application to Plane Surfaces

Next, suppose consideration is restricted to the case in which both the surface of the test piece and S_B are plane, and assume that the probes

are scanned in a plane parallel to S_B. Furthermore, assume that the test piece is much larger than the region containing the perturbation and that all fields are quasistatic. This means that, in the scan region, the fields generated by either probe in the absence of the perturbation are independent of the probe's position. Such a system is called shift invariant in optical system theory. If the signal generated by the perturbation (as the probes scan by) is call the observable image of the perturbation, then, as a result of shift invariance, this image can be deblurred (deconvolved) using Fourier-Transform theory. Equation (6) will be rewritten to show explicitly that it indeed has the form of a convolution integral.

Let the plane surface on S_B closest to the probes be an x-y plane located at the vertical coordinate, z. Also, let the origin of a coordinate system attached to the probes be (x_o,y_o,z_o). From the property of shift invariance, the fields generated by the probes in the unperturbed state will be functions only of $x-x_o$, $y-y_o$, and $z-z_o$. For the perturbed state, the fields on the upper part of S_B can be written in terms of their "incident" and "scattered" components, viz.,

$$\vec{E}_1(x,x_o,y,y_o) = \vec{E}_1^{\,o}(x-x_o,y-y_o)\cdot[\vec{\vec{I}} + \vec{\vec{S}}_E(x,y)] \qquad (7a)$$

$$\vec{H}_1(x,x_o,y,y_o) = \vec{H}_1^{\,o}(x-x_o,y-y_o)\cdot[\vec{\vec{I}} + \vec{\vec{S}}_H(x,y)] \quad . \qquad (7b)$$

Here, $\vec{E}_1^{\,o}$ and $\vec{H}_1^{\,o}$ are the unperturbed fields in Case 1, $\vec{\vec{I}}$ is the unit dyadic, and $\vec{\vec{S}}_{E,H}$ are dyadic scattering coefficients for the E and H fields. Note that, if S_B is very close to the physical perturbation in the test piece, these scattering coefficients are very localized in the x-y plane (a result of the quasistatic assumption). Dyadic scattering coefficients are used because, in general, cross-polarized coupling will occur. Given the boundary conditions on the test piece describing a particular perturbation, the electric and magnetic scattering coefficients can be related. It is these scattering coefficients (or their composite)

that will be called the electromagnetic near-field image of the perturbation.

If Eq. (7) is substituted into Eq. (6) and use is made of the fact that the integral over just the unperturbed fields must be zero, the following result is obtained:

$$v(x_o,y_o) = -(1/v_a I_b)\iint_{\text{all } xy} \{[\vec{E}_1^o(x-x_o,y-y_o)\cdot\overleftrightarrow{S}_E(x,y)]$$

$$\cdot[\vec{H}_2(x-x_o,y-y_o) \times \hat{n}] - [\vec{H}_1^o(x-x_o,y-y_o)\cdot\overleftrightarrow{S}_H(x,y)]$$

$$\cdot[\hat{n} \times \vec{E}_2(x-x_o,y-y_o)]\}\, dx\, dy \quad . \tag{8}$$

The integral can be extended over the entire x-y plane because the $\overleftrightarrow{S}_{E,H}$ are localized to a finite region of the top surface of S_B, and are zero outside that region.

Equation (8) has the form of a two-dimensional convolution. This result is easier to see if the special case of a one-dimensional perturbation is considered. Let the electric perturbation be a localized functon, $\beta(x)$, along the x direction and a constant in the y direction, and let the magnetic perturbation be negligible. Physically, such a perturbation might be a small slot or a step in a plane metal surface. In this case (since symmetry does not permit scattering in the y direction and there is negligible coupling to the y component of the electric field),

$$\overleftrightarrow{S}_E = \hat{i}\hat{i}\beta_{xx}(x) + \hat{i}\hat{k}\beta_{xz}(x) + \hat{k}\hat{i}\beta_{zx}(x) + \hat{k}\hat{k}\beta_{zz}(x) \quad . \tag{9}$$

Therefore,

$$\vec{E}_1^o \cdot \overleftrightarrow{S}_E = \hat{i}E_{1x}^o\, \beta_{xx}(x) + \hat{k}E_{1x}^o\, \beta_{xz}(x) + \hat{i}E_{1z}^o\, \beta_{zx}(x) + \hat{k}E_{1z}^o\, \beta_{zz}(x) \quad . \tag{10}$$

Also, since $\hat{n} = -\hat{k}$,

$$\vec{H}_2 \times \hat{n} = \hat{j}H_{2x} - \hat{i}H_{2y} \quad . \tag{11}$$

As a result,

$$[\vec{E}_1^o \cdot \overleftrightarrow{S}_E] \cdot [\vec{H}_2 \times \hat{n}] = -H_{2y}[E_{1x}^o \beta_{xx}(x) + E_{1z}^o \beta_{zx}(x)] \quad . \tag{12}$$

Finally, for simplicity, assume that $\beta_{zx} \approx 0$. Substitution into Eq. (8) gives

$$v(x_o) = (1/V_a I_b) \iint_{\text{all } xy} [E_{1x}^o(x-x_o, y-y_o) \cdot H_{2y}(x-x_o, y-y_o)] \beta_{xx}(x) \, dx \, dy \quad . \tag{13}$$

Equation 13 clearly has the form of a convolution. In this case, the line spread function of the probe system is defined as that function which, when convolved with $\beta_{xx}(x)$, produces the result given by Eq. (13). This function is

$$LS(x-x_o) = (1/V_a I_b) \int_{\text{all } y} [E_{1x}^o(x-x_o, y-y_o) \cdot H_{2y}(x-x_o, y-y_o)] \, dy \quad . \tag{14}$$

If the probes consist of coils whose axes are perpendicular to the plane surface, S_B, $LS(x-x_o)$ can be computed using the theory of Dodd and Deeds.[10] The mutual coupling present in Case 2 can also be included in the calculation if the source impedance, Z_a, is known.

The objective of this procedure is to estimate the improved "image", $\beta_{xx}(X)$, given the measured blurred "image", $v(x_o)$. This estimation can be done using Fourier-transform theory. Let $\tilde{V}(k)$, $\tilde{B}(k)$, and $\tilde{\tilde{LS}}(k)$ be the Fourier transforms of v, β_{xx}, and LS, respectively. Then, by the Convolution Theorem,

$$\tilde{V}(k) = \tilde{\tilde{LS}}(k) \cdot \tilde{B}(k) \quad . \tag{15}$$

The transform $\tilde{\tilde{LS}}$ represents a spatial filter. It must have an adequate spatial bandwidth if inversion of Eq. (15) is to produce a good "image" of β_{xx}.

In general, the near-field image of a perturbation that is localized in both x and y is determined by its point-spread function, rather than by the line-spread function discussed so far. An arbitrary electric perturbation produces six terms in Eq. (8), and a magnetic perturbation produces another six terms (some of these terms can be related, of course, if the boundary conditions describing the perturbation are known). Thus, a general near-field point-spread function is composed of a linear combination of products of the three components of electric field on S_B generated in Case 1 and the two tangential components of magnetic field generated in Case 2, plus a linear combination of products of the three components of magnetic field on S_B generated in Case 1 and the two tangential components of electric field generated in Case 2. All of these field components can be computed, say, for a Dodd-and-Deeds coil system. The observable image, v, is, in general, a sum of convolution integrals. Further work is required to determine how a meaningful near-field image can be obtained in this general case. However, there are practical cases of interest where enough special symmetries and approximations apply to make the near-field image concept immediately useful.

III SUMMARY

In summary, as a first step in the development of electromagnetic sensor arrays, a number of relative measurements of the responses of two-element sensor arrays (reflection probes) to steps and slots in aluminum plates have been made. These measurements have demonstrated the basic spatial characteristics of such arrays, and have been used successfully to validate a theoretical model for a reflection probe.

A survey of candidate technologies for fabricating high-resolution inductive electromagnetic sensor arrays has been initiated. One conclusion already drawn from this survey is that magnetic thin-film technology using printed coils is not particularly suitable for the NDE/robotics application. Thin-film magnetoresistive magnetic-field sensors appear more promising.

It may be possible to use generalized deconvolution procedures to enhance the spatial resolution of a given sensor array. Work has begun on the study of this possibility.

Future plans include continuing the evaluation of candidate technologies for fabricating complex sensor arrays with small elements, designing and testing an electronically scanned linear array, and developing imaging algorithms for such arrays.

APPENDIX A

A. Interactions

1. A. J. Bahr, "Electromagnetic Sensor Arrays--Experimental Studies," presented at the AFML/AFOSR contract review of NDE research, Ames Laboratory, University of Iowa, Ames, IA, April, 1985.

2. A. J. Bahr, "Electromagnetic Sensor Arrays--Experimental Studies," presented at the Review of Progress in Quantitative NDE, Williamsburg, VA, June, 1985. This paper will be published in the conference proceedings.

3. B. A. Auld and A. J. Bahr, "A Novel Multifunction Robot Sensor," to be presented at the 1986 IEEE International Conference on Robotics and Automation, San Francisco, CA, April, 1986.

B. Personnel

Dr. A. J. Bahr, Staff Scientist and Principal Investigator

Mr. R. D. Roach, Software Engineer

Mr. A. Rosengreen, Sr. Research Engineer

Mr. R. M. Ueberschaer, Research Engineer

Mr. W. B. Weir, Sr. Research Engineer

C. Acknowledgment

An extremely important element in this program is the close collaboration that exists between SRI personnel and Professor B. A. Auld and his students at Stanford University.

REFERENCES

1. B. A. Auld, J. Kenney, and T. Lookabaugh, "Electromagnetic Sensor Arrays--Theoretical Studies," Review of Progress in Quantitative Nondestructive Evaluation, Vol. 5, D. O. Thompson and D. E. Chimenti, Editors (Plenum Press, New York, 1985).

2. A. J. Bahr, "Electromagnetic Sensor Arrays--Experimental Studies," Review of Progress in Quantitative Nondestructive Evaluation, Vol. 5, D. O. Thompson and D. E. Chimenti, Editors (Plenum Press, New York, 1985).

3. J. P. Watjen and A. J. Bahr, "Evaluation of an Eddy-Current Tape-Head Probe," Review of Progress in Quantitative Nondestructive Evaluation, Vol. 3A, D. O. Thompson and D. E. Chimenti, Editors (Plenum Press, New York, 1984).

4. Y. Miura, et al., "Fabrication of Multi-Turn Thin Film Head," IEEE Trans. Magn., Vol. Mag-16, p. 779, (September 1980).

5. K. Yamada, et al., "Thin Film Head for High Density Magnetic Recording Using CoZr Amorphous Films," J. Appl. Phys., Vol. 55, p. 2235, (15 March 1984).

6. K. E. Kuijk, W. J. van Gestel and F. W. Gorter, "The Barber Pole, A Linear Magnetoresistive Head," IEEE Trans. Magn., Vol. Mag-11, p. 1215 (September 1975).

7. U. Dibbern, "The Amount of Linearization by Barber-Poles," IEEE Trans. Magn., Vol. Mag-20, p. 954 (September 1984).

8. W. Metzdorf, M. Beohner, and H. Handek, "The Design of Magnetoresistive Multitrack Read Heads for Magnetic Tapes," IEEE Trans. Magn., Vol. Mag-18, p. 763 (March 1982).

9. B. A. Auld, F. G. Meunnemann, and M. Riaziat, "Quantitative Modelling of Flaw Responses in Eddy Current Testing," Research Techniques in Nondestructive Testing, Vol. VII, R. S. Sharpe, Ed. (Academic Press, London, 1984).

10. C. V. Dodd and W. E. Deeds, "Analytical Solutions to Eddy-current Probe-Coil Problems," J. Appl. Phys., Vol. 33, pp. 2829-2839 (May 1968).


DAT
FILM